Science of the Total Environment 904 (2023) 166360

Contents lists available at ScienceDirect

Science of the Total Environment

journal homepage: www.elsevier.com/locate/scitotenv

Contrasting copper concentrations and isotopic compositions in two Great Lakes watersheds

Tassiane P. Junqueira [a], Daniel F. Araújo [b], Anna L. Harrison [c], Kaj Sullivan [a,d], Matthew I. Leybourne [a,e], Bas Vriens [a,*]

[a] Department of Geological Sciences and Geological Engineering, Queen's University, Kingston, Ontario, Canada
[b] Institut Français de Recherche pour l'Exploitation de la Mer (IFREMER), Brest, France
[c] Geoscience Environment Toulouse, National Scientific Research Centre (CNRS), Toulouse, France
[d] Department of Chemistry, Ghent University, Ghent, Belgium
[e] Arthur B. McDonald Canadian Astroparticle Physics Research Institute, Department of Physics, Engineering Physics and Astronomy, Queen's University, Kingston, Ontario, Canada

HIGHLIGHTS

- High-resolution hydrogeochemical analysis of two Great Lakes catchments
- Analysis of $\delta^{65}Cu$ signatures in >25 rock, soil, and surface water samples
- Mining-derived dissolved Cu isotopic composition traceable >30 km from source
- Spatially diffuse isotope patterns complicate Cu source attribution in Trent River.

GRAPHICAL ABSTRACT

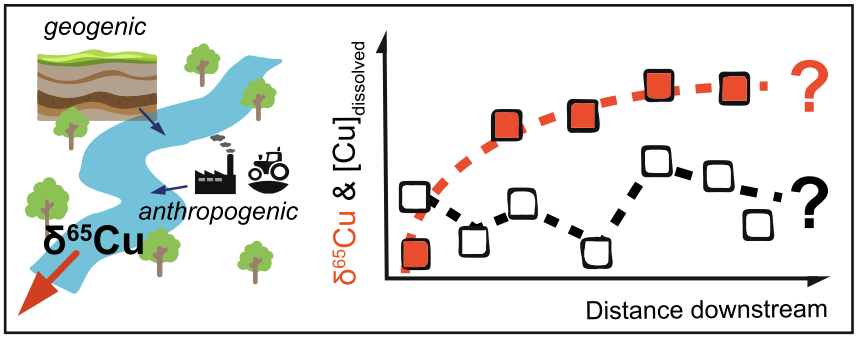

ARTICLE INFO

Editor: José Virgílio Cruz

Keywords:
Great Lakes
Copper
Metal contaminants
Stable isotopes
Source tracking

ABSTRACT

Copper (Cu) stable isotopes can elucidate the biogeochemical controls and sources governing Cu dynamics in aquatic environments, but their application in larger rivers and catchments remains comparatively scarce. Here, we use major and trace element hydrogeochemical data, Cu isotope analyses, and mixing modeling, to assess Cu loads and sources in two major river systems in Ontario, Canada. In both the Spanish River and Trent River catchments, aqueous hydrochemical compositions appeared reasonably consistent, but Cu concentrations were more variable spatially. In the Spanish River, waters near (historic) industrial mining activities displayed positive Cu isotope compositions ($\delta^{65}Cu_{SRM\text{-}976}$ between +0.75 ‰ and +1.01 ‰), but these signatures were gradually attenuated downstream by mixing with natural background waters ($\delta^{65}Cu$ −0.65 ‰ to −0.16 ‰). In contrast, Trent River waters exhibited more irregular in-stream Cu isotope patterns ($\delta^{65}Cu$ from −0.75 ‰ to +0.21 ‰), beyond the variability in Cu isotope signatures observed for adjacent agricultural soils ($\delta^{65}Cu$ between −0.26 ‰ and +0.30 ‰) and lacking spatial correlation, reflective of the more diffuse sourcing and entwined endmember contributions to Cu loads in this catchment. This work shows that metal stable isotopes may improve our understanding of the sources and baseline dynamics of metals, even in large river systems.

* Corresponding author.
E-mail address: bas.vriens@queensu.ca (B. Vriens).

https://doi.org/10.1016/j.scitotenv.2023.166360
Received 17 May 2023; Received in revised form 18 July 2023; Accepted 15 August 2023
Available online 16 August 2023

1. Introduction

Copper (Cu) is an important trace metal and essential micronutrient for organisms, but it can also be toxic to humans and other biota when present at elevated concentrations. Copper is naturally present and bioavailable in soils and surface waters from processes such as rock and soil weathering or atmospheric deposition (Sullivan et al., 2022; Leybourne and Cameron, 2008), but Cu concentrations may also be increased because of human activity, including through point sources like metal mining and smelting, logging and pulp processing, infrastructure, and industrial manufacturing (Daehn et al., 2017; Kerfoot et al., 1999; Sivry et al., 2008; Yin et al., 2015), as well as through diffuse sources such as application of Cu-based pesticides and fungicides (Vázquez-Blanco et al., 2022; Droz et al., 2021) and urban runoff (Ancion et al., 2010). The relevance of these potential geogenic versus anthropogenic Cu sources is highly variable spatiotemporally, with confounding impacts on Cu occurrence in surface environments (Fitchko and Hutchinson, 1975; Sullivan et al., 2022). In addition, the occurrence and fate of Cu in surface waters, particularly at baseline levels, is intricately coupled to low-temperature inorganic processes (physicochemical mineral-fluid interactions) and biological scavenging, and, therefore, the prevailing redox conditions and availability of macronutrients and primary production (Thomas et al., 2017; Schoenfuss et al., 2020). A multitude of sources and biogeochemical processes thus need to be considered to understand Cu distribution patterns in surface waters (Fekiacova et al., 2015).

Copper stable isotope variations in natural samples can be comparatively large relative to their mass difference (Wiederhold, 2015) and have been used as effective tracers of biogeochemical reactions and for source attribution in various environments, including seawater (Takano et al., 2017; Vance et al., 2008), freshwaters such as lakes, wetlands, and rivers (Babcsányi et al., 2014; Sivry et al., 2008), soils (Fekiacova et al., 2015; Babcsányi et al., 2016), lacustrine and marine sediments (Little et al., 2014; Nitzsche et al., 2021; Araújo et al., 2017, 2019a, 2019b), atmospheric aerosols (Yang et al., 2019; Souto-Oliveira et al., 2019) and road dust (Jeong and Ra, 2021). Vance et al. (2008) presented an extensive dataset for Cu isotopic compositions in rivers worldwide, revealing a range in dissolved δ^{65}Cu values from +0.02 to +1.45 per mil (‰, relative to NIST SRM-976). Open ocean waters generally exhibit Cu isotopic compositions heavier than those of rivers (δ^{65}Cu + 0.9 ± 0.5 ‰), possibly related to fractionation during biological scavenging or aqueous complexation (Little et al., 2014; Takano et al., 2017; Baconnais et al., 2019). Recently, Wang et al. (2020) investigated δ^{65}Cu of dissolved Cu in the Yangtze River and tributaries, which appeared higher than that of other rivers and was influenced by streamflow management and the presence of Cu sulfide deposits. In addition, various authors leveraged Cu isotopes to constrain the importance of mining as a source of Cu contamination in surface waters (Borrok et al., 2008; Kimball et al., 2009; Viers et al., 2018; Su et al., 2018). However, the applicability of Cu isotope analyses in other riverine environments, especially hydrodynamically complex catchments, is otherwise scarce: the isotopic patterns of Cu have been studied predominantly in Cu-contaminated or enriched systems, whereas data from more pristine rivers is lacking.

The North American Great Lakes form a globally unique freshwater resource, consisting of five major, serially connected lakes that are fed by thousands of tributaries across the United States and Canada (Sterner et al., 2017). Since the industrial revolution, anthropogenic emissions of metals have caused environmental degradation at various locations in the Great Lakes, particularly in the so-called Areas-of-Concern (Hartig et al., 2020). Copper is among the main historically important metal contaminants in the Great Lakes region (Chapra et al., 2012), but much of the information available on the sources and behavior of Cu in the Great Lakes is consequently derived from studies conducted in these locations with Cu-enriched sediments and/or waters, including the Hamilton Harbour, Spanish Harbour, and Bay of Quinte (Crowder et al., 1989; Dixit et al., 1998; Milani et al., 2017). A recent mass-balance assessment of basin-scale Cu loads in the Great Lakes has revealed variable source-sink behavior across the individual lakes, and suggested that atmospheric deposition, natural riverine runoff, and sedimentation, may all significantly impact lake-wide Cu budgets (Bentley et al., 2022). Nevertheless, the sources and (baseline) dynamics of Cu in other Great Lakes areas, including in most major tributaries, remain enigmatic.

Two catchments in the Great Lakes region with significant Cu loads include the Spanish River (~12 t Cu/yr discharged to the Georgian Bay and Lake Huron), and the Trent River (~4 t Cu/yr discharged to Lake Ontario; Bentley et al., 2022). Both rivers are similar in terms of average summer flowrate (90 m^3/s for the Spanish River, 120 m^3/s for the Trent River; Environment and Climate Change Canada (ECCC), 2016) and catchment size (12,400 km^2 for the Trent River, 14,000 km^2 for the Spanish River; NRCAN database - Natural Resources Canada database, n. d.), but their catchment's geological backgrounds, land use statistics, and (low) population densities (~90 versus 45 people/km^2 for the Trent and Spanish Rivers, respectively) are dissimilar. The Spanish River and its major tributary, the Vermillion River, are situated in late Archean to Paleoproterozoic bedrock dominated by Ni-Cu-enriched felsic-intrusive and metamorphic rocks (Sudbury Igneous Complex; Gartner et al., 1980), whereas most of the Trent River basin is underlain by the Mesoproterozoic Canadian Shield in the north and mid-Ordovician limestones in the south (Brennand and Shaw, 1994; Brookfield and Brett, 1987). The Vermillion River catchment further includes Sudbury, a city known for major Ni—Cu mining and metallurgical activities since the early 1900's (Adamo et al., 1996); mining in the Sudbury district has been an important source of Ni and Cu enrichment in sediments in the Spanish Harbour, a historically contaminated site at the mouth of the Spanish River that is currently in recovery (Dixit et al., 1998). However, the relative present contributions of geogenic versus anthropogenic Cu loads in the Spanish River remain unknown (Bentley et al., 2022). In contrast, the Trent River drains the sparsely populated Kawartha Lakes and supplying watersheds in the northern part of its basin but has a significant agricultural region in its southern portion (32 % of the basin's land coverage is pasture and cropland). Further, much of the Trent River downstream of the fluvial mid-catchment Rice Lake is part of an engineered waterway containing >15 canal locks and hydroelectric dams. Potential sources of Cu in this catchment may thus include natural weathering of Cu-bearing surficial deposits and soils, as well as anthropogenic inputs from industry, small population centers, or application of agricultural amendments (Sullivan et al., 2022), but their relative significance remains to be determined. Quantifying the origins and biogeochemical cycling of Cu in these large catchments (i.e., discharge >50 m^3/s) with distinctively different potential point- versus non-point sources is imperative for our understanding of Cu dynamics in the Great Lakes basin and natural river systems in general.

To this end, we investigate the hydrochemistry and Cu isotope signatures in the Trent and Spanish River basins, as well as in a selection of possible endmember source materials in a first attempt to screen the potential range of isotopic signatures in these complex systems. The observed spatial trends in Cu loading rates and isotope compositions are used in mixing models to examine anthropogenic versus natural sources, as well as biogeochemical processes affecting Cu dynamics in these two catchments.

2. Materials and methods

2.1. Field sampling

Surface waters from 35 locations in the Trent River catchment and 25 locations in the Spanish River catchment (Fig. 1) were sampled in August 2021, well after snowmelt and avoiding major rain events. A subset of 16 samples were strategically selected posteriorly for isotope analysis, to ensure spatial coverage of the catchments, including at major tributary confluences. Surface water sampling locations, coordinates, and dates are provided in Table S1. During the sampling

campaign, weather conditions (temperature, precipitation) were typical for the respective regions in August (Table S2).

Surface water samples were collected using a roped, 20 L metal-free low-density polyethylene (LDPE) Niskin-type bucket from the stream centerlines (nominal depth of <1 m), to obtain a well-mixed sample with minimal suspension of particulates. Duplicates were collected in select locations to ensure repeatability. Immediately upon collection, aqueous samples were subdivided into 3 aliquots: (i) 250 mL was filtered using 0.25 μm PTFE syringe filters (VWR, Canada) and acidified to 1 % nitric acid (HNO_3) using ultrapure HNO_3 (trace element grade, Sigma Aldrich) for analysis of total cation concentrations, (ii) 250 mL was filtered as per (i) but not acidified for analysis of anions and electrochemical parameters, and (iii) 1 L bulk water (unfiltered and unacidified) was express-shipped to the laboratory for filtering and acidification before

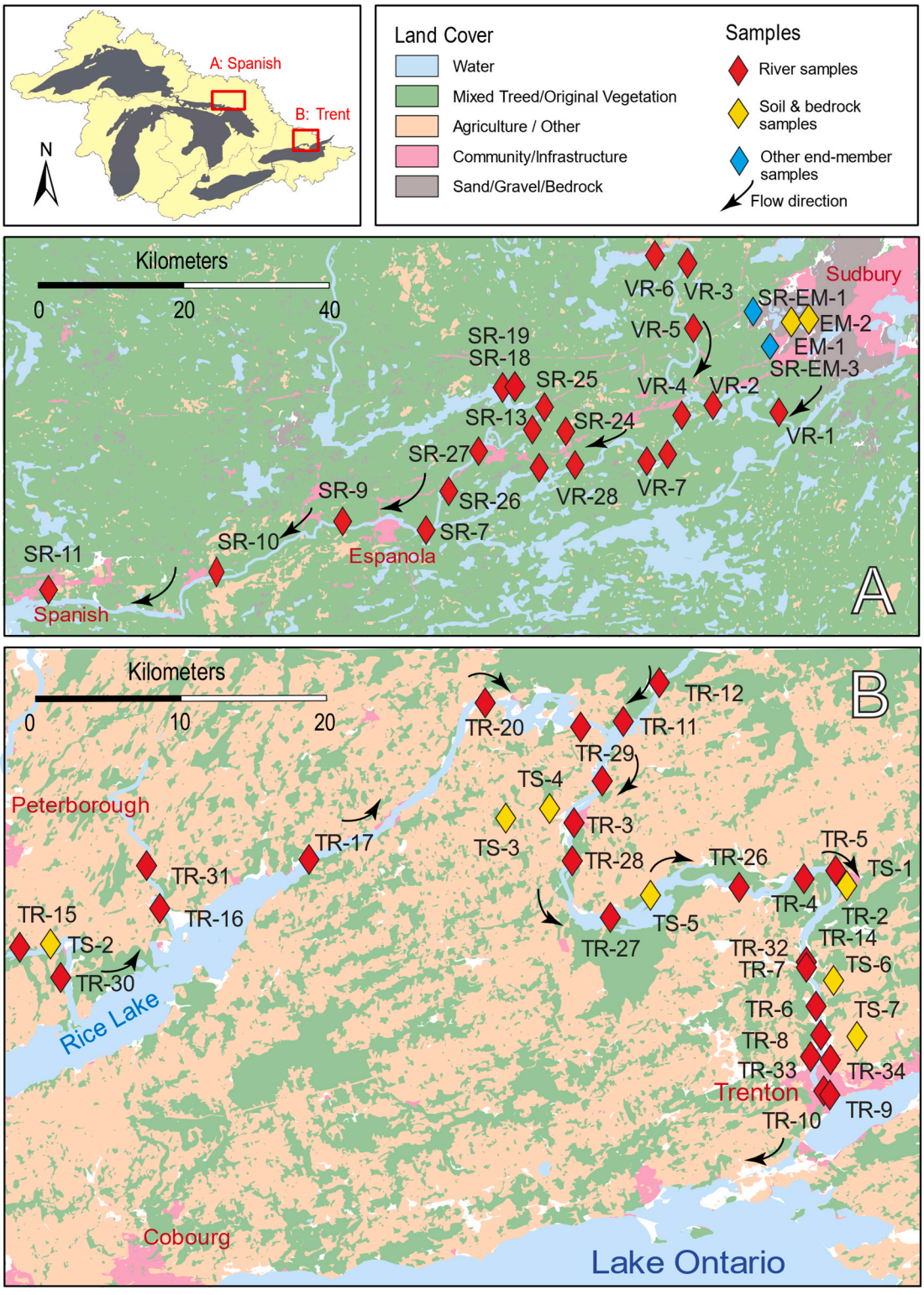

Fig. 1. Sampling locations and land cover in the Spanish River (A; top) and Trent River (B; bottom) catchments (individual spatial scales), Ontario, Canada. The location of both catchments within the Great Lakes region is indicated in the top left; the land cover and sampling legend in the top right applies to both frames.

purification for Cu isotope analysis (Section 2.2). All aqueous sample aliquots were stored in opaque Nalgene bottles (TraceCert, Supelco) in an ice-packed cooler at <4 °C in the dark until further processing. Sample handling equipment was pre-cleaned with 2 % ultrapure HNO_3 and de-ionized (DI) water (18.2 MΩ; Millipore Q-pod) before use, and five control samples per catchment (DI water blanks) were collected as described above for procedural blanks. The remainder of the collected sample was used to measure electrochemical parameters in the field (temperature, pH, redox potential [ORP], total dissolved solids [TDS], specific conductance [EC], and dissolved oxygen [DO]), using HANNA HI9813-6 multimeters, Milwaukee MW500 Portable ORP meters, and Extech DO-210 Dissolved Oxygen probes. All field probes were calibrated per manufacturer instructions every five samples.

Six bedrock samples were collected as grab samples at accessible and exposed locations after dislodging with a rock hammer. After consideration of previous geological mapping (Lightfoot and Farrow, 2002) and representative bulk elemental composition, two bedrock samples were selected for isotope analysis. Top-soil samples ($n = 7$) were collected from select agricultural fields for which permission was obtained, and which were proximal (<2 km) to the main river branch and strategically spread across the catchment. Top-soils were sampled using a 3 cm diameter soil auger to a maximum depth of 30 cm (A and B soil horizons). For each soil sample, material was collected at four different sub-locations spread ~50 m across a single field plot, which was cleared from macroscopic crop residue, if needed, and subsequently mixed and homogenized. All collected rock and soil samples were stored in plastic ZipLock bags and kept at <4 °C in the dark until further processing. The sampling locations of these soil and rock samples, as well as two mine waste seepage samples collected as stream samples as described above, are detailed in Table S3.

2.2. Sample processing

Aqueous sample aliquots for isotope analysis were vacuum-filtered through 0.25 μm nylon membrane filters (ChromTech, Canada) in the laboratory immediately upon receipt. For this, an acid-washed glass vacuum-filtration apparatus was operated inside a custom-built Plexiglas chamber that allowed for controlled internal air circulation through a HEPA filter, and the Plexiglas chamber itself was situated in an over-pressurized Class-1000 clean room at the Queen's Facility for Isotope Research (QFIR, Queen's University, Canada). Blanks (DI water) and duplicates were generated every 10 samples for procedural quality control on the filtration process. The obtained filtered aliquots were subsequently acidified to 2 % with ultrapure HNO_3, evaporated to obtain approximately 250 ng of Cu (typically requiring 100–1000 mL of aqueous sample) and pre-purified for isotope analysis in an over-pressurized class-1000 clean room at the Queen's University Nano-Fabrication Kingston (NFK) center (Section 2.3.2). Duplicates and triplicates of select samples were processed depending on availability of sample volume.

Rock samples were fragmented to <1 mm diameter using a SelFrag electric pulse crusher (SelFrag AG, Switzerland). Crushed bedrock and collected soil samples were then freeze-dried (Freezone −50 °C, LabConco) for 24 h, and ground with an agate mortar and pestle. Dried and crushed solid samples were subsequently acid-digested in an aqua-regia-like solution in a Multiwave 3000 microwave-assisted digestor (Anton-Paar). For this, 3 mL HNO_3, 9 mL hydrochloric acid (HCl), 2 mL hydrogen peroxide (H_2O_2), and 3 mL hydrofluoric acid (HF) were added to ~50 mg sample aliquots weighed into Teflon-PFA vessels and heated at 240 °C for 4 h. All acids (47 % HF, OmniTrace, 67 % HNO_3, Anachemia, and 37 % HCl, Fisher Chemical) and the peroxide (32 % H_2O_2, VWR Avantor) were of ultrapure grade. Following digestion, acid extracts were cooled for 60 min and transferred to pre-cleaned Falcon tubes and diluted to a final volume of 50 mL with DI water. Aliquots of the final digestates were analyzed for total elemental concentrations and Cu isotopic composition (Section 2.3). Two blanks and three commercially available certified matrix reference materials (VHG-SL1, sewage sludge, VHG-SSD-1A, soil, and USGS-BHVO-1, Hawaiian basalt) were included with each digestion cycle. The average recovery of Cu was 107 ± 2 % across these three solid reference materials (Table S4).

2.3. Analytical methodology

2.3.1. Total elemental concentrations and major water quality parameters

Total concentrations of Cu and other trace elements in aqueous samples and acid-digestates were measured on an iCAP triple quadrupole-inductively coupled plasma-mass spectrometer (TQ-ICP-MS; Thermo Scientific). The instrument was operated as a single quadrupole in KED mode (He collision gas) or as a triple-quadrupole (O_2 reaction gas), utilizing mass shifting to reduce isobaric interferences. Major elements, including Na, Ca, Mg, S, and P, were also quantified using a Thermo Scientific iCAP Pro XPS inductively coupled plasma-optical emission spectrometer (ICP-OES). Both instruments were externally calibrated daily, and internal standards (Sc, In, Re) were used for drift correction. Analytical blanks and commercial aqueous certified reference materials (NRC-AQUA1, NRC-SLRS-6, and NIST-1643f) were measured every $n = 10$ samples (average elemental recovery 96 ± 11 %; Table S5). Finally, dissolved ion concentrations of sulfate (SO_4^{-2}), phosphate (PO_4^{-3}), chloride (Cl^-), as well as total carbonate alkalinity, were measured on an automated photospectrometer (ThermoScientific Gallery) using supplier reagents and instructions. Detection limits are provided in Table S6.

2.3.2. Sample pre-purification for isotope analysis

Sample pre-purification and reagent preparation for isotope analysis occurred in a laminar flow hood in a Class-1000 clean room at Queen's University's NFK center. Ultrapure HCl and HNO_3 for sample purification were distilled by sub-boiling technical grade acids (VWR, ACS Grade) on a DST-1000 (Savillex) purification system and titration with 18.2 MΩ DI water (Millipore Q-pod). The sample pre-purification methodology was adapted from Maréchal et al. (1999), Kidder et al. (2020), and Sullivan et al. (2020), and is summarized in Table S7. In brief, Cu was isolated from the aqueous sample matrix using 8 mm Teflon columns (Eichrom Technologies Inc.) loaded with 1 mL pre-cleaned Bio-Rad AG MP-1 strong exchange resin (100–200 mesh). Before sample loading, the resin was cleaned with 20 mL 3 M HNO_3, 20 mL 6 M HCl, and 20 mL DI water, after which the column was conditioned with 4 mL 8 M HCl. The samples were loaded onto the resin in 1 to 2 mL 8 M HCl + 0.03 % H_2O_2. Matrix elements were first removed using 4 mL 8 M HCl + 0.03 % H_2O_2, Cu was eluted in 13 mL of 8 M HCl + 0.03 % H_2O_2, after which Fe and Zn were collected in 10 mL 1 M HCl + 0.03 % H_2O_2, and 10 mL DI water, respectively, all in pre-cleaned Savillex Teflon vials. The collected fractions were subsequently evaporated on a hotplate (80 °C) for 24 h in the clean room, re-dissolved in 1 mL 8 M HCl and re-loaded onto the column for a second pass, and third pass for select samples with high matrix element concentrations. For these second and third purification steps, the column resin preparation and elution steps were the same as those of the first pass (Table S7). A synthetic multi-element solution containing Cu, Na, Ti, Fe, Zn, and other matrix elements at concentrations of 10 μg/mL was used for optimization and quality-control of the pre-purification; the achieved chromatographic separation of Cu from the sample matrix is illustrated in Fig. S1. The chromatographic recovery yield of samples was checked before isotope analysis to exclude isotope bias from purification.

2.3.3. Copper isotope analysis

Pre-purified sample collects were first refluxed in their Savillex vials with 50 μL concentrated HNO_3 on a hotplate (180 °C), and subsequently evaporated at 80 °C and re-dissolved in 300 μL of 2 % HNO_3 to break down organic residues from the resin and replace matrix chlorides with nitrates for analysis. Copper isotope abundances were subsequently determined on a Neptune or Neptune+ multicollector-ICP-MS (MC-ICP-

MS; both ThermoScientific) in wet-plasma mode, either at QFIR (Queen's University, Kingston, Canada), at the PSO (Ocean Spectrometry Pole) platform at L'Institut Français de Recherche pour l'exploitation de la Mer (IFREMER; Brest, France), or at Géosciences Environnement Toulouse (GET; France). Pre-purified samples with Cu concentrations of ~250 ng were introduced to the MC-ICP-MS through an Elemental Scientific microFast dual-loop syringe-injection autosampler, a low-flow (20–50 μL/min) PFA nebulizer, and cyclonic double-pass quartz spray chamber. Copper isotopic compositions are reported as δ^{65}Cu values relative to NIST SRM-976, as follows:

$$\delta^{65}Cu(‰) = \left[\frac{\left(\frac{Cu^{65}}{Cu^{63}}\right)_{sample}}{\left(\frac{Cu^{65}}{Cu^{63}}\right)_{standard}} - 1 \right] \times 1000$$

Measured Cu isotope ratios were corrected for instrumental mass bias by performing sample standard bracketing with the isotopic standards ERM-AE633 and NIST SRM-976 (Kidder et al., 2020). Aqueous and solid samples for which repeat analyses failed to achieve a standard deviation of ±0.08 ‰ were not further considered or interpreted. Finally, multiple certified reference materials were used for methodological validation of the Cu isotope analyses. These included BIR-1 and BHVO-1 (USGS; basalt), SLRS-4-6 (NRC; rivers water), MESS-3-4 (NRC; marine sediment), and SSD-1A (VHG; amended soil, first report). The δ^{65}Cu values determined for these reference materials are reported and compared with literature values in Table S8.

2.4. Data processing

Copper enrichment factors in soil samples were calculated based on aluminum- and titanium-normalized Cu concentration ratios of samples compared to the respective ratios of appropriate backgrounds, as described in Supporting Information Methods M1 and Table S9. Finally, isotope mixing models were constructed with IsoSource (Version 1.3.1, US Environmental Protection Agency) to calculate the ranges of potential endmember contributions to stable isotope mixtures (river water samples), as described in Supporting Information Methods M2 and Table S10.

3. Results and discussion

3.1. Hydrochemistry of the Spanish and Trent Rivers

All Spanish and Trent River water samples were well-oxygenated (5.4 mg/L < O_2 < 10.7 mg/L; corroborated by ORP values >125 mV), neutral to slightly alkaline (6.6 < pH < 8.9) and had alkalinity between 58 mg/L to 222 mg/L (Table S11). Both rivers exhibited consistently low phosphate concentrations at <15 μg/L, on average. Whereas sulfate and chloride levels were reasonably consistent in the Trent River (<35 % relative standard deviation across the catchment), they varied significantly in the Spanish River, e.g., from <4 to >40 mg/L for both sulfate and chloride (Table S11). The Spanish River further contained on average higher concentrations of Ca, Mg, Al, and sulfate than the Trent River, but lower alkalinity and lower concentrations of Na, Cl, and Si (p values between 0.01 and 0.1); Table S11), in line with the different geological backgrounds and population densities of these catchments (Thurston et al., 1992); a Piper diagram illustrating the general river water types is provided in Fig. S2. Overall, dissolved chloride, phosphate, and sulfate concentrations determined by photospectrometry quantitatively aligned with total dissolved Cl, P, and S concentrations obtained by ICP-OES or ICP-MS (data not shown), confirming these ions dominated the aqueous speciation of these elements. Assessment of the ion charge balance of the river samples revealed only minor excess positive charge (<5 meq/L; data not shown), which is attributed to the fact that negatively charged dissolved organic matter, nitrogen species, and halogens other than chloride were not measured. Further, a comparison between the recorded hydrochemistry and surface water quality data from the Ontario Provincial Water Quality Monitoring Network (PWQMN - Provincial Water Quality Monitoring, n.d.; Table S12) shows that aqueous parameters in 2021 were generally in line with long-term averages.

In addition to differences between the Spanish and Trent Rivers, water quality also varied within each catchment. The majority of water quality parameters measured within the Trent River was fairly normally distributed (skewness<|1.6|), but variability in the Spanish River was higher (skewness>3 for various parameters; Table S11). There were no discernable spatial trends of consistently increasing or decreasing major or trace element concentrations upstream-to-downstream in either river. At least part of the observed variability in water quality is attributed to the distribution of sampling locations: the Trent River was sampled more predominantly in its main branch, and its sampled tributaries displayed a similar hydrochemistry, with the exception of slightly higher Cl in the Crowe River and slightly higher sulfate in the Indian and Otonabee Rivers. In contrast, the Spanish River sampling locations included more tributaries that exhibited higher phosphate and chloride concentrations (i.e., up to 3 times the Spanish River average in Junction Creek), or higher sulfate, Ca, and alkalinity (e.g., in the Black and Ministic Creeks, and, to a lesser extent, Vermillion River). Overall, the major water quality parameters thus reveal reasonably consistent water types in the Spanish and Trent River catchments, overprinted by hydrochemical variability introduced by tributaries.

3.2. Trends in dissolved Cu in the Spanish and Trent rivers

Dissolved Cu concentrations in the Trent River ranged from 0.2 to 2.5 μg/L and in the Spanish River from 0.8 to 4.9 μg/L (Fig. 2), both of which are in line with ranges observed in long-term monitoring programs (Table S12). Whereas the Cu concentrations recorded in both river systems were spatially variable across their entire catchments, they did not reveal a consistent trend of accumulation or depletion upstream-to-downstream (Fig. 2). On average, dissolved Cu concentrations in the Spanish River (2.5 ± 1.4 μg/L) were significantly ($P < 0.01$) higher than in the Trent River (0.9 ± 0.1 μg/L), but the overall variability in these concentrations was lower in the Spanish River than in the Trent River (skewness of 0.3 compared to 1.1 in Trent River; Table S11). Dissolved Cu concentrations between neighboring sampling locations changed only slightly for the Spanish River (<20 % per km), but more substantially for the Trent River (up to a factor of 4 per km). The few samples with relatively high Cu did not exclusively correspond to locations near urban areas (e.g., TR9 in Trenton or VR1 near Sudbury), nor to specific sampled tributaries (e.g., TR31 in the Indian River): elevated Cu concentrations were equally recorded in the main branches of both rivers (Fig. 2).

A comparison between Cu concentrations and other hydrochemical parameters reveals that elevated Cu concentrations in specific locations in both the Spanish and Trent Rivers were unrelated to anomalies in other major parameters (examples in Fig. S3). With the exception of the elevated solute levels in the Junction Creek sample near Sudbury, tributary and main branch samples with elevated Cu concentrations in both rivers appeared to have hydrochemical compositions typical for their respective catchments (Table S11). This lack of systematic and significant Cu enrichment in the sampled tributaries suggests that confluences are not a major control on Cu dynamics in these catchments, especially when considering their smaller flow rates and therefore Cu loads. The reasonably consistent Spanish and Trent River hydrochemistry discussed above, including in terms of phosphate (Table S11), further implies that in-stream variability in biogeochemical cycling of Cu is small, but additional analysis of other parameters (nitrogen, chlorophyll) is required to confirm. Finally, the absence of precipitation events during sampling rules out dilution effects on the observed Cu concentration dynamics.

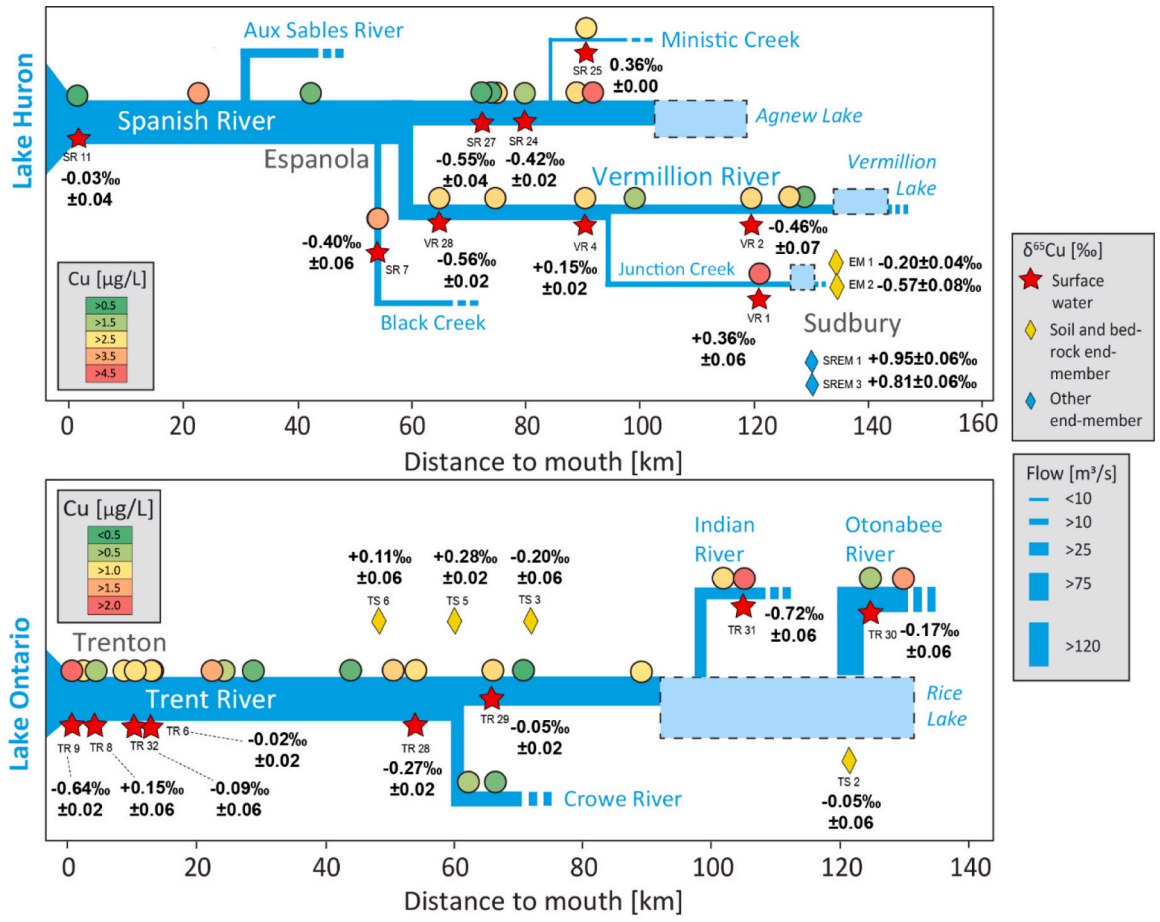

Fig. 2. Spatial trends of total dissolved Cu concentrations and δ^{65}Cu values in the Spanish and Trent River catchments. Plotted against the distance-to-river-mouth (x-axes) for the two river systems are the total concentrations of Cu in the Spanish River (top panel) and Trent River (bottom panel) systems, with the sampling locations indicated by the color-coded circles (corresponding legends indicated in each frame), as well as Cu isotope compositions of river water samples and endmember samples in both catchments (right legend applies to both frames). The approximate average flow rate is identified by stream thickness (right legend; both frames) and major hydrological features are annotated for clarity.

The spatially variable occurrence of Cu in the Trent and Spanish River systems may have been influenced by other natural and anthropogenic inputs, including unsampled tributaries (albeit with small discharge), wastewater treatment effluents (e.g., near Sudbury; Pinter et al., 2022), or baseflow. For the latter, groundwater data for both catchments are scarce, but monitoring through the Ontario Provincial Groundwater Monitoring Network (PGMN – Provincial Groundwater Monitoring Network, n.d.) suggests that groundwater Cu levels were consistent between 2006 and 2019 and ranged between 0.8 and 4.9 µg/L for select wells near Sudbury (Spanish River) and between 0.3 and 2.2 µg/L in select wells across the lower Trent River basin (Table S13). Groundwater Cu concentrations are thus similar to those observed in nearby surface water samples and display a similar spatial variability. However, further speculation on the potential role of groundwater discharge in controlling surface water Cu levels is complicated by the lack of monitoring data for surficial aquifers in other regions of these catchments, particularly the sparsely populated upper reaches of both catchments, as well as uncertainty in the location of gaining versus losing stream segments. The suggested role of groundwater for solute dynamics in other areas of the Great Lakes (Xu et al., 2021) warrants additional investigation of the baseline groundwater chemistry, including for Cu, and especially in upstream regions of the Spanish and Trent River watersheds. In summary, dissolved Cu concentrations were consistently higher in the Spanish River compared to the Trent River ($p < 0.01$), but in both cases, Cu occurrence patterns are spatially variable and lack correlation with other major hydrochemical parameters.

3.3. Chemical composition of soils, rocks, and mine waste seepage

The elemental composition of the sampled solid materials and mine waste seepage is provided in Table S14. Bedrock samples from the Spanish River basin contained lithologies representative of the area (Sudbury Igneous Complex; Lightfoot and Farrow, 2002), including partially melted and brecciated footwall gneisses with complex sulfide mineralization and platinum group element-rich mineralization (Morris et al., 2022). The total Cu content in these bedrock samples ranged between 2.8 and 4.2 mg/kg, and showed high contents of Cu, Zn, and S (Table S14), albeit at lower magnitudes than the average grade in Sudbury Igneous Complex rocks (~1 % Cu; Lightfoot and Farrow, 2002). Aqueous samples collected in mine waste seepage streams near Sudbury were acidic ($2.8 < pH < 5.8$) and contained up to 1.6 mg/L dissolved Cu, as well as high (mg/L-range) levels of other solutes, including sulfate, Fe, and Zn (Table S14). These seepage waters thus display features resemblant of acid rock drainage, with high dissolved Cu concentrations sustained by low pH and a composition markedly different from other creeks sampled in the Spanish River catchment.

Soil samples collected across the Trent River catchment exhibited Cu contents from 8 to 47 mg/kg (Table S14); a range similar to previous data for sediments in this region (Frank et al., 1976). Soils with higher Cu contents were not co-located to river locations with elevated dissolved Cu concentrations. Further, Cu contents were correlated ($R^2 = 0.81$) with the P contents of the agricultural soil samples (between 0.47 and 3.16 mg/kg), as well as with other major elements (e.g., Na or Fe at

$R^2 > 0.65$; Table S14). Calculated enrichment factors (EF) for the soil samples ranged between 0.4 and 1.2, overall (Table S9), suggesting that the agricultural soils collected in the Trent River catchment present little to no Cu enrichment. The samples with the largest EF (TS6 and TS3 at 1.22 and 1.02, respectively) did not have the highest Cu content (Table S14), were located at opposite ends of the sampled region (Fig. 1) and did not coincide with river locations with elevated dissolved Cu. Soil samples TS1 and TS2 exhibited the lowest Cu content, as well as the lowest EF, indicating that these samples may be representative of the geogenic background. In context of much higher EF of Cu reported for other soils and sediments (Araújo et al., 2017; Thapalia et al., 2010), the soils sampled in the Trent River catchment thus do not demonstrate a significant enrichment of Cu.

3.4. Copper isotopic signatures

The δ^{65}Cu values measured for the Spanish and Trent River water samples, as well as for bedrock and soil endmember samples, are provided in Fig. 2 and Table S15. Overall, significant variability in δ^{65}Cu was observed across samples within both catchments; a general comparison of the entire dataset with previously published δ^{65}Cu values for rivers is provided in Fig. S4. Trends in Cu isotope signatures in both catchments are discussed separately below.

3.4.1. Copper isotope compositions in the Spanish River system

Bedrock samples from the Spanish River basin displayed slightly negative δ^{65}Cu values (−0.57 ± 0.08 ‰ to −0.20 ± 0.04 ‰; Fig. 3, Table S15), aligning with previous data on similar, mafic metamorphized rocks (−0.69 to −0.20 ‰; Zhao et al., 2022) and showing a depletion of ^{65}Cu relative to the upper continental crust (UCC; δ^{65}Cu + 0.07 ‰; Li et al., 2009). In contrast, the mine waste seepage samples presented more positive δ^{65}Cu values ranging from +0.81 to +0.95 ‰ (2SD of ±0.06 ‰; $n = 6$), showing an enrichment of ^{65}Cu in the seepage relative to the bedrock. Previous work on Cu isotopes in natural archives impacted by mining and metallurgical wastes has found large variability in δ^{65}Cu in fluids (−1.52 ‰ to +1.75 ‰; Viers et al., 2018; Song et al., 2016; Sullivan et al., 2022), a range which the mine waste seepage samples from this work fall within. The oxidative dissolution of Cu-bearing sulfides underlying acid rock drainage and subsequent retention of Cu in secondary precipitates may render the Cu isotopic composition of affected seeps enriched in the heavier Cu isotope relative to the original solid (Viers et al., 2018; Masbou et al., 2020). Thus, the ^{65}Cu-enriched mine wastewater samples may represent the endmember contribution of mining activities to the Junction Creek and therefore the Spanish River, whereas the ^{65}Cu depleted bedrocks may be considered more representative of the geogenic endmember.

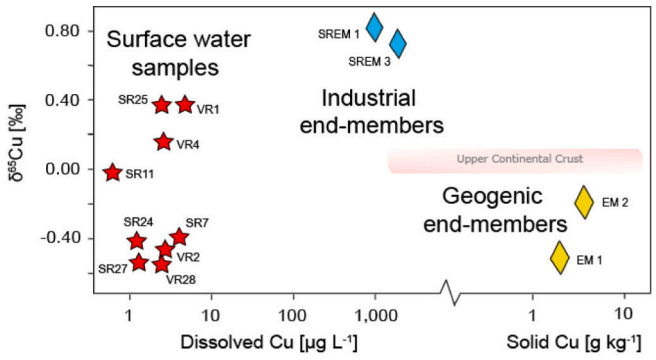

Fig. 3. Copper isotopic compositions (δ^{65}Cu; ‰) versus Cu concentrations for Spanish River water samples and investigated endmember materials. Raw data is provided in Tables S11 and S14. The Upper Continental Crust value is obtained from Li et al. (2009); δ^{65}Cu ~ 0.07 ‰. Surface water samples are indicated in red stars, industrial (mine wastewater) endmembers in blue, and geogenic endmembers (natural bedrock) in yellow rhombuses, all with sample numbers indicated adjacent to the symbols. Note the truncated x-axes to visualize dissolved- versus solid-phase Cu concentrations.

Stream water samples collected in the Spanish River displayed a large upstream-to-downstream variation of δ^{65}Cu values from −0.56 to +0.36 ‰ (Fig. 3, Table S15). The Cu isotope composition of stream water proximal to tailings (VR1 and VR4) was significantly enriched in ^{65}Cu (+0.15 to +0.36 ‰), above the signature of the upper continental crust but below those of the mine waste seepage samples. The isotope compositions of waters sampled in non-impacted locations in the Black Creek (sample SR7) and Vermilion River (sample VR2, Fig. 2) were more negative than −0.40 ± 0.07 ‰, indicating Cu in upstream uncontaminated areas is depleted in ^{65}Cu relative to the mine wastewater seepage and more in line with the bedrock background (Fig. 3). Thus, the distinct separation in dissolved δ^{65}Cu signatures in Spanish River water samples suggests that surface waters emanating near mine waste storage facilities carry a distinctive "heavy" isotopic fingerprint compared to more pristine waters that are less likely to be influenced by anthropogenic activities and instead carry a ^{65}Cu/^{63}Cu ratio close to that of the regional bedrock (Fig. 3).

To further assess the above hypothesis, mixing models were used to estimate the potential source proportions of mine waste seepage in four increasingly downstream Spanish River water mixtures (VR1, VR4, VR28, and SR11; Methods M2). The mixing calculations predict an average mine-derived Cu source proportion of ~60 % at VR1 in Junction Creek, which decreases to ~3 % further downstream in the Vermillion River (VR28; Fig. S5). The average discharge of the Junction Creek near Sudbury is 5–10 m^3/s (ECCC, 2016) and measured Cu concentrations are on the order of a few µg/L (VR1; Table S10), indicating that any inputs with Cu concentrations exceeding 1 mg/L, as is the case for the mine waste seepages, need only exhibit very small flow rates (on the order of 10–100 L/s) to achieve a 60 % overall Cu load contribution. These discharge rates are realistic for the sampled mine waste seepage creeks. At VR28, >40 km downstream of VR1, the Vermillion River has flow rates of >50 m^3/s, but the predicted source proportion of the mine waste seepage also quantitatively supports its gradual dilution considering the Cu load at this location (Table S10). An exception is the most downstream Spanish River sample SR11 with slightly elevated δ^{65}Cu values relative to the geogenic background. For this location, the mixing model predicted unrealistically high source proportions (Fig. S5), given that the discharge at the mouth of the Spanish River is ~150 m^3/s. We speculate that the isotopic composition of this sample is potentially affected by backflow, or that its (low) dissolved Cu concentrations are impacted by re-suspension or upward diffusion of sediment-derived Cu. However, overall, the gradual mixing of the mine-derived Cu load carried by the Junction Creek with downstream tributaries after transecting the Sudbury district may explain the observed decrease in the δ^{65}Cu values for ~40 km in the Vermillion River, with downstream persistence being dependent on the magnitude of the source load and the absence of other sources of significant scale in the catchment.

Finally, once introduced to surface water, dissolved Cu may fractionate as a result of biological uptake (Ryan et al., 2013), mineral precipitation (e.g., in acid mine drainage settings; Viers et al., 2018), or adsorption (Sullivan et al., 2022). Except for the most upstream sample VR1, the consistently near-neutral, oxic, and low TDS conditions in the Spanish River are not indicative of strong redox gradients that could have induced extensive precipitation and thereby Cu isotopic fractionation. This is further corroborated by a lack of systematic variation in δ^{65}Cu as a function of pH, alkalinity or ORP (Fig. S3). The consistent hydrochemistry in the Spanish River main branch, in addition to relatively short transport times, thus suggests that the variability in its Cu isotopic composition, including the gradually decreasing upstream-to-downstream signature, is source-determined and practically conservative with little fractionation post-solubilization. However, additional time-resolved analyses of river waters and endmember materials like groundwaters are required to further elucidate such in-stream Cu isotope dynamics.

3.4.2. Copper isotope compositions in the Trent River system

Measured δ^{65}Cu values for samples of soils collected >50 km apart throughout the Trent River catchment varied between −0.20 and +0.28 ‰ (Fig. 4 and Table S15). The variability and overlapping Cu isotopic compositions of these (non-enriched) soils are consistent with the broader ranges of δ^{65}Cu values observed in non-contaminated soils elsewhere (Bigalke et al., 2010, 2011; Thapalia et al., 2010; Sullivan et al., 2022). The soil sample with the highest Cu content (TS5; 48 mg/kg) in the Trent River catchment exhibited the most positive Cu isotope signature (+0.28 ‰), but the soil with highest Cu enrichment factor (TS3; up to 3.6; minor enrichment) exhibited the lowest δ^{65}Cu value (−0.20 ‰; Fig. 4). No correlations between δ^{65}Cu and the Cu concentration nor the Cu enrichment factor were evident, unlike what has been observed in contaminated sediments elsewhere (Araújo et al., 2019a, 2019b; Fekiacova et al., 2015). The absence of such relationships is likely due to the limited number of samples analyzed, the relatively low Cu contents and enrichment factors in the soils of this study, and the fact that Cu occurrence in soil environments is generally affected by many factors, including the aqueous and mineralogical chemical speciation of Cu and alteration thereto under variable soil redox conditions and horizontal/vertical deportment, all of which affect Cu isotope signatures in soils (Bigalke et al., 2010, 2011; Kusonwiriyawong et al., 2017; Wang et al., 2017). In addition, soil composition data may be normalized to the parent material (e.g., as in Mathur et al., 2012) however, unweathered bedrock for the Trent basin was not collected in the present work.

The δ^{65}Cu range of Trent River water samples (δ^{65}Cu ranging from −0.72 to +0.15 ‰; Fig. 4) overlapped with that of the investigated soils in the catchment, but with higher variability and trending to more negative values. No consistent upstream-to-downstream trends in Cu isotopic composition could be observed in the Trent River water samples (Fig. 2; Table S15). Furthermore, δ^{65}Cu values in Trent River water samples appeared unrelated to pH, alkalinity, or ORP (Fig. S3), or to concentrations of other major ions, including phosphate and sulfate (data not shown). The aqueous Cu isotope compositions also did not systematically correlate with δ^{65}Cu values of nearby soil samples (e.g., soil sample TS6 exhibited a different δ^{65}Cu (+0.11 ‰) than the <2 km upstream surface water sample TR32 (−0.02 ‰); Fig. 2).

The geology and land use characteristics of the Trent River catchment are considerably more heterogeneous than those of the Spanish River (Fig. 1) and this catchment heterogeneity implies that Cu may be released from different and more diffuse sources along the river flow path. In order to investigate the potential source proportions of soil endmembers to Cu dynamics in Trent River surface waters, mixing models were constructed to quantify the widest possible range of source-mixing solutions able to explain the observed δ^{65}Cu values (Methods M2; Table S10). The mixing calculations show that the most positive aqueous δ^{65}Cu value in Trent River sample TR8 (+0.15 ‰) can be explained by soil sample contributions of up to 60 % from the most positive and negative δ^{65}Cu soils (TS5; +0.28 ± 0.02 ‰, and TS3; −0.20 ± 0.06 ‰, respectively; Fig. S6), and similarly, that negative aqueous δ^{65}Cu values for the Trent River main branch (sample TR28; −0.27 ± 0.01 ‰) can be produced by soil sample contributions of up to 30 %, using the same most positive and negative soil δ^{65}Cu values. Furthermore, adoption of a literature δ^{65}Cu value for pesticides (−0.49 ± 0.01 ‰; Blotevogel et al., 2018) shows similarly wide-ranging potential source contributions of 28–42 %, on average, for the most positive and negative δ^{65}Cu values in Trent River water samples, respectively (Fig. S6). These improbable and impractically large ranges in source proportions suggest that the overlapping δ^{65}Cu values for even a single endmember type (soils), and potential myriad of other entwined Cu sources contributing to the riverine Cu isotope signature, prohibit a further tracing of its exact sourcing in this catchment.

Although the reasonably consistent hydrochemical composition of the Trent River water samples (similar to the Spanish River discussed above) equally suggest little in-stream Cu fractionation upstream-to-downstream, the imprints of more diffuse Cu sources in the Trent River catchment, as well as biogeochemical Cu fractionation along the soil-groundwater and groundwater-surface water interfaces (Vázquez-Blanco et al., 2022), remain elusive. Thus, the reported data show that for larger-scale heterogeneous river systems, in order to use Cu isotopes for source-tracking, it is critical to have well-defined endmembers and quantitative constraints on potential fractionation processes at the soil-river interface and within catchment reservoirs (e.g., in Rice Lake in the Trent River catchment). Additional stable isotopic systems such as Zn, Cd, or Li, may be complementary tools (Fekiacova et al., 2015; Millot and Négrel, 2021).

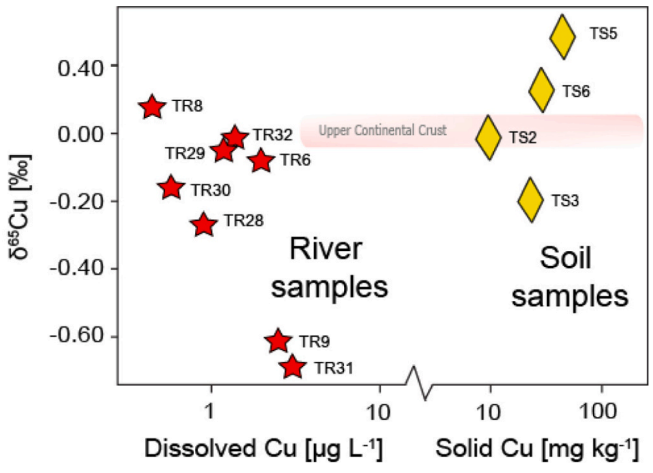

Fig. 4. Copper isotopic compositions (δ^{65}Cu; ‰) versus Cu concentrations for Trent River water samples and investigated endmember materials. Raw data is provided in Tables S11 and S14. The Upper Continental Crust value is obtained from Li et al. (2009); δ^{65}Cu ~ 0.07 ‰. River water samples are indicated as red stars, endmembers (soils) in yellow rhombuses, all with sample numbers indicated adjacent to the symbols. Note the truncated x-axes to visualize dissolved- versus solid-phase Cu concentrations.

3.5. Implications for water quality management

Copper isotopic analysis has been successfully applied to source-track Cu inputs in smaller-scale catchments with distinct endmember signatures (e.g., Cobica River, Spain; Viers et al., 2018; Meca River, Spain, Masbou et al., 2020), but have been less applied in rivers with >100 m^3/s discharge rates. This study presented new Cu isotope data for major fluvial systems in the Great Lakes basin. The Cu isotope composition of Spanish River headwaters was significantly enriched in ^{65}Cu relative to the average bedrock in the catchment, and imprints on the downstream river could be tracked to significant (>30 km) distance. Our work provides additional evidence for a genetic link between continued Cu loads to the Spanish River and (historic) mining activities in the Sudbury district and suggests that Cu isotopes can be applied to source-track loads in other mining-impacted rivers, even when discharge rates are high and the river network complex. For the Trent River, catchment heterogeneity, diffuse Cu sourcing and overlapping endmember signatures prevented a conclusive causal assessment of surface water Cu isotope compositions and the investigated soil endmembers. Additional sampling and analysis of endmember materials (i.e., wastewater effluent, urban runoff, road dust), as well as quantification of Cu fractionation at the soil-river interface, could aid investigations of Cu dynamics in this catchment.

Despite dissolved Cu concentrations in the Spanish and Trent River systems remaining below water quality guidelines, both rivers introduce Cu to their receiving Great Lakes with basin-relevant loads (Bentley et al., 2022). The Spanish and Trent Rivers displayed downstream δ^{65}Cu compositions between −0.03 ‰ and − 0.64 ‰ (Fig. 2, Table S15), suggestive of major inputs of ^{65}Cu-depleted riverine Cu to Lakes Huron and Ontario. Further investigation of Cu isotope patterns in the

connecting channels of the Great Lakes basin, including in the St. Lawrence River, may help elucidate whether the observed Spanish and Trent River tributary signatures extrapolate to basin-scale Cu export and align with other global river systems (Vance et al., 2008), or whether additional in-lake fractionation occurs and can be used to refine estimates of Cu loading rates delivered to the Atlantic Ocean. Identifying these pathways and sources by which Cu is transported into and across the Great Lakes will improve water quality management at transnational scale, for historically contaminated sites as well as regional baseline levels. Furthermore, this study demonstrates a means to fingerprint Cu sources in materials that may possess relatively low concentrations, which may be applied to other river systems to refine global baseline levels or to examine regional impacts of anthropogenic (e.g., mining) activities.

CRediT authorship contribution statement

Tassiane P. Junqueira: Methodology, Validation, Investigation, Data curation, Writing – original draft. **Daniel F. Araújo:** Methodology, Validation, Writing – review & editing. **Anna L. Harrison:** Investigation, Supervision, Writing – review & editing. **Kaj Sullivan:** Methodology, Investigation, Writing – review & editing. **Matthew I. Leybourne:** Investigation, Supervision, Writing – review & editing. **Bas Vriens:** Investigation, Supervision, Writing – review & editing, Project administration.

Declaration of competing interest

The authors declare the following financial interests/personal relationships which may be considered as potential competing interests: Bas Vriens reports financial support was provided by National Science and Engineering Research Council (NSERC) Canada.

Data availability

Data will be made available on request.

Acknowledgements

We thank Graham Gibson (NFK) for clean room assistance, and Colton Bentley, Nima Saberi, and Jaabir Ali (Queen's University) for help with field sampling. Cassidy Theodoro-Neville (Queen's University) is acknowledged for sample processing, and James Kidder, Alexandre Voinot, Donald Chipley, Marissa Valentino (Queen's University Facility for Isotope Research), Klervia Jaouen, Jérôme Chmeleff, and Vasileios Mavromatis (GET Toulouse), and Jeong Hyeryeong (IFREMER, Nantes) for assistance with elemental and isotope analyses. Financial support was provided by Queen's University, the Natural Science and Engineering Research Council of Canada (NSERC; grant number 2021-00244), and the Canadian Foundation for Innovation (CFI; grant number 38468). Leybourne acknowledges funding from the Canada First Research Excellence Fund through the Arthur B. McDonald Canadian Astroparticle Physics Research Institute.

Appendix B. Supplementary data

The Supplementary Information (Supporting Methods M1-M2, Fig. S1-S6 and Tables S1-S15) contains additional methodology on calculation of enrichment factors and isotope mixing modeling, sampling location details and analytical quality control, as well as additional results, including data on river hydrochemistry and endmember composition and their Cu isotope signatures. Supplementary data to this article can be found online at doi:https://doi.org/10.1016/j.scitotenv.2023.166360.

References

Adamo, P., Dudka, S., Wilson, M.J., McHardy, W.J., 1996. Chemical and mineralogical forms of Cu and Ni in contaminated soils from the Sudbury mining and smelting region, Canada. Environ. Pollut. 91 (1), 11–19. https://doi.org/10.1016/0269-7491(95)00035-P.

Ancion, P.Y., Lear, G., Lewis, G.D., 2010. Three common metal contaminants of urban runoff (Zn, Cu and Pb) accumulate in freshwater biofilm and modify embedded bacterial communities. Environ. Pollut. 158 (8), 2738–2745. https://doi.org/10.1016/j.envpol.2010.04.013.

Araújo, D.F., Boaventura, G.R., Viers, J., Mulholland, D.S., Weiss, D., Araújo, D., Lima, B., Ruiz, I., Machado, W., Babinski, M., Dantas, E., 2017. Ion exchange chromatography and mass bias correction for accurate and precise Zn isotope ratio measurements in environmental reference materials by MC-ICP-MS. J. Braz. Chem. Soc. 28 (2), 225–235. https://doi.org/10.5935/0103-5053.20160167.

Araújo, D.F., Ponzevera, E., Briant, N., Knoery, J., Bruzac, S., Sireau, T., Brach-Papa, C., 2019a. Copper, zinc and lead isotope signatures of sediments from a mediterranean coastal bay impacted by naval activities and urban sources. Appl. Geochem. 111, 104440 https://doi.org/10.1016/j.apgeochem.2019.104440.

Araújo, D.F., Ponzevera, E., Briant, N., Knoery, J., Sireau, T., Mojtahid, M., Metzger, E., Brach-Papa, C., 2019b. Assessment of the metal contamination evolution in the Loire estuary using Cu and Zn stable isotopes and geochemical data in sediments. Mar. Pollut. Bull. 143, 12–23. https://doi.org/10.1016/j.marpolbul.2019.04.034.

Babcsányi, I., Imfeld, G., Granet, M., Chabaux, F., 2014. Copper stable isotopes to trace copper behavior in wetland systems. Environ. Sci. Technol. 48 (10), 5520–5529. https://doi.org/10.1021/es405688v.

Babcsányi, I., Chabaux, F., Granet, M., Meite, F., Payraudeau, S., Duplay, J., Imfeld, G., 2016. Copper in soil fractions and runoff in a vineyard catchment: insights from copper stable isotopes. Sci. Total Environ. 557-558, 154–162. https://doi.org/10.1016/j.scitotenv.2016.03.037.

Baconnais, I., Rouxel, O., Dulaquais, G., Boye, M., 2019. Determination of the copper isotope composition of seawater revisited: a case study from the Mediterranean Sea. Chem. Geol. 511, 465–480. https://doi.org/10.1016/j.chemgeo.2018.09.009.

Bentley, C., Junqueira, T., Dove, A., Vriens, B., 2022. Mass-balance modeling of metal loading rates in the Great Lakes. Environ. Res. 205, 112557 https://doi.org/10.1016/j.envres.2021.112557.

Bigalke, M., Weyer, S., Kobza, J., Wilcke, W., 2010. Stable Cu and Zn isotope ratios as tracers of sources and transport of Cu and Zn in contaminated soil. Geochim. Cosmochim. Acta 74 (23), 6801–6813. https://doi.org/10.1016/j.gca.2010.08.044.

Bigalke, M., Weyer, S., Wilcke, W., 2011. Stable Cu isotope fractionation in soils during oxic weathering and podzolization. Geochim. Cosmochim. Acta 75 (11), 3119–3134. https://doi.org/10.1016/j.gca.2011.03.005.

Blotevogel, S., Oliva, P., Denaix, L., Audry, S., Viers, J., Schreck, E., 2018. Stable Cu isotope ratios show changes in Cu uptake and transport mechanisms in Vitis vinifera due to high Cu exposure. Front. Plant Sci. 12, 755944 https://doi.org/10.3389/fpls.2021.755944.

Borrok, D.M., Nimick, D.A., Wanty, B.W., Ridley, W.I., 2008. Isotopic variations of dissolved copper and zinc in stream waters affected by historical mining. Geochim. Cosmochim. Acta 72 (2), 329–344. https://doi.org/10.1016/j.gca.2007.11.014.

Brennand, T., Shaw, J., 1994. Tunnel channels and associated landforms: their implication for ice sheet hydrology. Can. J. Earth Sci. 31, 502–522. https://doi.org/10.1139/e94-045.

Brookfield, M.E., Brett, C.E., 1987. Paleoenvironments of the Mid-Ordovician (Upper Caradoxian) Trenton limestones od southern Ontario, Canada: storm sedimentation on a shoal-basin shelf model. Sediment. Geol. 57, 75–105. https://doi.org/10.1016/0037-0738(88)90019-X.

Chapra, S.C., Dove, A., Warren, G.J., 2012. Long-term trends of Great Lakes major ion chemistry. J. Great Lakes Res. 38 (3), 550–560. https://doi.org/10.1016/j.jglr.2012.06.010.

Crowder, A., Dushenko, W.T., Greig, J., Poland, J.S., 1989. Metal contamination in sediments and biota of the Bay of Quinte, Lake Ontario, Canada. In: Environmental Bioassay Techniques and their Application: Proceedings of the 1st International Conference held in Lancaster, England, 11–14 July 1988 (pp. 337-343). Springer Netherlands. https://doi.org/10.1007/978-94-009-1896-2_31.

Daehn, K.E., Serrenho, A.C., Allwood, J.M., 2017. How will copper contamination constrain future global steel recycling? Environ. Sci. Technol. 51 (11), 6599–6606. https://doi.org/10.1021/acs.est.7b00997.

Dixit, A.S., Dixit, S.S., Smol, J.P., Keller, W.B., 1998. Paleolimnological study of metal and nutrient changes in Spanish harbour, North Channel of Lake Huron (Ontario). Lake Reserv. Manag. 14 (4), 428–439. https://doi.org/10.1080/07438149809354349.

Droz, B., Payraudeau, S., Rodriguez Martin, J.A., Tóth, G., Panagos, P., Montanarella, L., Imfeld, G., 2021. Copper content and export in European vineyard soils influenced by climate and soil properties. Environ. Sci. Technol. 55 (11), 7327–7334. https://doi.org/10.1021/acs.est.0c02093.

ECCC - Environment and Climate Change Canada, 2016. Climate Data and Scenarios for Canada: Synthesis of Recent Observation and Modelling Results. Available online: http://publications.gc.ca/pub?id=9.809265andsl=0 (Accessed March 2023).

Fekiacova, Z., Cornu, S., Pichat, S., 2015. Tracing contamination sources in soils with Cu and Zn isotopic ratios. Sci. Total Environ. 517, 96–105. https://doi.org/10.1016/j.scitotenv.2015.02.046.

Fitchko, J., Hutchinson, T.C., 1975. A comparative study of heavy metal concentrations in river mouth sediments around the Great Lakes. J. Great Lakes Res. 1 (1), 46–78. https://doi.org/10.1016/S0380-1330(75)72335-3.

Frank, R., Ishida, K., Suda, P., 1976. Metals in agricultural soils of Ontario. Can. J. Soil Sci. 56, 181–196. https://doi.org/10.4141/cjss76-027.

Gartner, J.F., Mollard, J.D., Roed, M.A., 1980. Ontario Engineering Geology Terrain Study Users' Manual; Ontario Geological Survey, Open File Report 5288, 99 p. Available online: http://www.geologyontario.mndm.gov.on.ca/.

Hartig, J.H., Krantzberg, G., Alsip, P., 2020. Thirty-five years of restoring Great Lakes areas of concern: gradual progress, hopeful future. J. Great Lakes Res. 46, 429–442. https://doi.org/10.1016/j.jglr.2020.04.004.

Jeong, H., Ra, K., 2021. Characteristics of potentially toxic elements, risk assessments, and isotopic compositions (Cu-Zn-Pb) in the PM10 fraction of road dust in Busan, South Korea. Atmosphere 12 (9), 1229. https://doi.org/10.3390/atmos12091229.

Kerfoot, W.C., Harting, S., Rossmann, R., Robbins, J.A., 1999. Anthropogenic copper inventories and mercury profiles from Lake Superior: evidence for mining impacts. J. Great Lakes Res. 25 (4), 663–682. https://doi.org/10.1016/s0380-1330(99)70769-0.

Kidder, J.A., Voinot, A., Sullivan, K.V., Chipley, D., Valentino, M., Layton-Matthews, D., Leybourne, M., 2020. Improved ion-exchange column chromatography for Cu purification from high-Na matrices and isotopic analysis by MC-ICPMS. J. Anal. At. Spectrom. 35, 776–783. https://doi.org/10.1039/C9JA00359B.

Kimball, B.E., Mathur, R., Dohnalkova, A.C., Wall, A.J., Runkel, R.L., Brantley, S.L., 2009. Copper isotope fractionation in acid mine drainage. Geochim. Cosmochim. Acta 73 (5), 1247–1263. https://doi.org/10.1016/j.gca.2008.11.035.

Kusonwiriyawong, C., Bigalke, M., Cornu, S., Montagne, D., Fekiacova, Z., Lazarov, M., Wilcke, W., 2017. Response of copper concentrations and stable isotope ratios to artificial drainage in a French Retisol. Geoderma 300, 44–54. https://doi.org/10.1016/j.geoderma.2017.04.003.

Leybourne, M.I., Cameron, E.M., 2008. Source, transport, and fate of rhenium, selenium, molybdenum, arsenic, and copper in groundwater associated with porphyry-Cu deposits, Atacama Desert, Chile. Chem. Geol. 247 (1–2), 208–228. https://doi.org/10.1016/j.chemgeo.2007.10.017.

Li, W., Jackson, S.E., Pearson, N.J., Alard, O., Chappell, B.W., 2009. The Cu isotopic signature of granites from the Lachlan Fold Belt, SE Australia. Chem. Geol. 258 (1–2), 38–49. https://doi.org/10.1016/j.chemgeo.2008.06.047.

Lightfoot, P.C., Farrow, C.E., 2002. Geology, geochemistry, and mineralogy of the Worthington offset dike: a genetic model for offset dike mineralization in the Sudbury Igneous Complex. Econ. Geol. 97 (7), 1419–1446. https://doi.org/10.2113/gsecongeo.97.7.1419e.

Little, S.H., Vance, D., Walker-Brown, C., Landing, W.M., 2014. The oceanic mass balance of copper and zinc isotopes, investigated by analysis of their inputs, and outputs to ferromanganese oxide sediments. Geochim. Cosmochim. Acta 125, 673–693. https://doi.org/10.1016/j.gca.2013.07.046.

Maréchal, C.N., Télouk, P., Albarède, F., 1999. Precise analysis of copper and zinc isotopic compositions by plasma-source mass spectrometry. Chem. Geol. 156 (1–4), 251–273. https://doi.org/10.1016/S0009-2541(98)00191-0.

Masbou, J., Viers, J., Grande, J.A., Freydier, R., Zouiten, C., Seyler, P., de la Torre, M.L., 2020. Strong temporal and spatial variation of dissolved Cu isotope composition in acid mine drainage under contrasted hydrological conditions. Environ. Pollut. 266, 115104 https://doi.org/10.1016/j.envpol.2020.115104.

Mathur, R., Jin, L., Prush, V., Paul, J., Eberole, C., Fornadel, A., Williams, J.Z., Brantley, S., 2012. Cu isotopes and concentrations during weathering of black shale of the Marcellus Formation, Huntingdon County, Pennsylvania (USA). Chem. Geol. 304-305, 175–184. https://doi.org/10.1016/j.chemgeo.2012.02.015.

Milani, D., Grapentine, L., Burniston, D.A., Graham, M., Marvin, C., 2017. Trends in sediment quality in Hamilton Harbour, Lake Ontario. Aquat. Ecosyst. Health Manag. 20 (3), 295–307. https://doi.org/10.1080/14634988.2017.1302780.

Millot, R., Négrel, P., 2021. Lithium isotopes in the Loire River Basin (France): hydrogeochemical characterizations at two complementary scales. Appl. Geochem. 125, 104831 https://doi.org/10.1016/j.apgeochem.2020.104831.

Morris, W.A., Underhay, S.L., Ugalde, H., 2022. Morphology and tectonic modification of the Sudbury Impact Crater-The North Range. Can. J. Earth Sci. https://doi.org/10.1139/cjes-2022-0066.

Nitzsche, K.N., Yoshimura, T., Ishikawa, N.F., Ogawa, N.O., Suzuki, K., Ohkouchi, N., 2021. Trace metal geochemical and Zn stable isotope data as tracers for anthropogenic metal contributions in a sediment core from Lake Biwa, Japan. Appl. Geochem. 134, 105107 https://doi.org/10.1016/j.apgeochem.2021.105107.

NRCAN database - Natural Resources Canada database. Available online. https://natural-resources.canada.ca/science-and-data/21444 (accessed April 2023).

PGMN – Provincial Groundwater Monitoring Network. Publicly available data. https://data.ontario.ca/dataset/provincial-groundwater-monitoring-network (Accessed April 2023).

Pinter, J., Jones, B.S., Vriens, B., 2022. Loads and elimination of trace elements in wastewater in the Great Lakes basin. Water Res. 209, 117949 https://doi.org/10.1016/j.watres.2021.117949.

PWQMN - Provincial Water Quality Monitoring. Publicly Available Data. https://datastream.org/dataset/f3877597-9114-4ace-ad6f-e8a68435c0ba (Accessed April 2023).

Ryan, B.M., Kirby, J.K., Degryse, F., Harris, H., McLaughlin, M.J., Scheiderich, K., 2013. Copper speciation and isotopic fractionation in plants: uptake and translocation mechanisms. New Phytol. 199 (2), 367–378. https://doi.org/10.1111/nph.12276.

Schoenfuss, H.L., Wang, L.C., Korn, V.R., King, C.K., Kohno, S., Hummel, S.L., 2020. Understanding the ecological consequences of ubiquitous contaminants of emerging concern in the Laurentian Great Lakes watershed: a continuum of evidence from the laboratory to the environment. In: Crossman, J., Weisener, C. (Eds.), Contaminants of the Great Lakes. The Handbook of Environmental Chemistry. Springer, p. 101. https://doi.org/10.1007/698_2020_491.

Sivry, Y., Riotte, J., Sonke, J.E., Audry, S., Schafer, J., Viers, J., Blanc, G., Freydier, R., Dupré, B., 2008. Zinc isotopes as tracers of anthropogenic pollution from Zn-ore smelters: the Riou Mort-Lot River system. Chem. Geol. 255, 295–304. https://doi.org/10.1016/j.chemgeo.2008.06.038.

Song, S., Mathur, R., Ruiz, J., Chen, D., Allin, N., Guo, K., Kang, W., 2016. Fingerprinting two metal contaminants in streams with Cu isotopes near the Dexing Mine, China. Sci. Total Environ. 544, 677–685. https://doi.org/10.1016/j.scitotenv.2015.11.101.

Souto-Oliveira, C.E., Babinski, M., Araújo, D.F., Weiss, D.J., Ruiz, I.R., 2019. Multi-isotope approach of Pb, Cu and Zn in urban aerosols and anthropogenic sources improves tracing of the atmospheric pollutant sources in megacities. Atmos. Environ. 198, 427–437. https://doi.org/10.1016/j.atmosenv.2018.11.007.

Sterner, R.W., Ostrom, P., Ostrom, N.E., Klump, J.V., Steinman, A.D., Dreelin, E.A., Fisk, A.T., 2017. Grand challenges for research in the Laurentian Great Lakes. Limnol. Oceanogr. 62 (6), 2510–2523. https://doi.org/10.1002/lno.10585.

Su, J., Mathur, R., Brumm, G., D'Amico, P., Godfrey, L., Ruiz, J., Song, S., 2018. Tracing copper migration in the Tongling area through copper isotope values in soils and waters. Int. J. Environ. Res. Public Health 15 (12), 2661. https://doi.org/10.3390/ijerph15122661.

Sullivan, K.V., Layton-Matthews, D., Leybourne, M., Kidder, J., Mester, Z., Yang, L., 2020. Copper isotopic analysis in geological and biological reference materials by MC-ICP-MS. Geostand. Geoanal. Res. 44, 349–362. https://doi.org/10.1111/ggr.12315.

Sullivan, K.V., Kidder, J.A., Junqueira, T.P., Vanhaecke, F., Leybourne, M.I., 2022. Emerging applications of high-precision Cu isotopic analysis by MC-ICP-MS. Sci. Total Environ. 838, 156084 https://doi.org/10.1016/j.scitotenv.2022.156084.

Takano, S., Tanimizu, M., Hirata, T., Shin, K.C., Fukami, Y., Suzuki, K., Sohrin, Y., 2017. A simple and rapid method for isotopic analysis of nickel, copper, and zinc in seawater using chelating extraction and anion exchange. Anal. Chim. Acta 967, 1–11. https://doi.org/10.1016/j.aca.2017.03.010.

Thapalia, A., Borrok, D.M., Metre, P.C.V., Musgrove, M., Landa, E.R., 2010. Zn and Cu isotopes as tracers of anthropogenic contamination in a sediment core from an urban lake. Environ. Sci. Technol. 44 (5), 1544–1550. https://doi.org/10.1021/es902933y.

Thomas, L.M., Jorgenson, Z.G., Brigham, M.E., Choy, S.J., Moore, J.N., Banda, J.B., Gefell, D., Minarik, T.A., Schoenfuss, H.L., 2017. Contaminants of emerging concern in tributaries to the laurentian great lakes: II. Biological consequences of exposure. PLoS One 12 (9), e0182868. https://doi.org/10.1371/journal.pone.0182868.

Thurston, P.C., Williams, H.R., Sutcliffe, R.H., Stott, G.M., 1992. Geology of Ontario; Ontario Ministry of Northern Development and Mines, Ontario Geological Survey Special, Volume 4, 1525 p. ISBN-10: 0772989753.

Vance, D., Archer, C., Bermin, J., Perkins, J., Statham, P.J., Lohan, M.C., Ellwood, M.J., Mills, R.A., 2008. The copper isotope geochemistry of rivers and the oceans. Earth Planet. Sci. Lett. 274 (1–2), 204–213. https://doi.org/10.1016/j.epsl.2008.07.026.

Vázquez-Blanco, R., Nóvoa-Muñoz, J.C., Arias-Estévez, M., Fernández-Calviño, D., Pérez-Rodríguez, P., 2022. Changes in Cu accumulation and fractionation along soil depth in acid soils of vineyards and abandoned vineyards (now forests). Agric. Ecosyst. Environ. 339, 108146 https://doi.org/10.1016/j.agee.2022.108146.

Viers, J., Grande, J.A., Zouiten, C., Freydier, R., Masbou, J., Valente, T., Torre, M.L., Destrigneville, C., Pokrovsky, O.S., 2018. Are Cu isotopes a useful tool to trace metal sources and processes in acid mine drainage (AMD) context? Chemosphere 193, 1071–1079. https://doi.org/10.1016/j.chemosphere.2017.11.133.

Wang, P., Dong, G., Santosh, M., Liu, K., Li, X., 2017. Copper isotopes trace the evolution of skarn ores: a case study from the Hongshan-Hongniu Cu deposit, southwest China. Ore Geol. Rev. 88, 822–831. https://doi.org/10.1016/j.oregeorev.2016.11.023.

Wang, Q., Zhou, L., Little, S.H., Liu, J., Feng, L., Tong, S., 2020. The geochemical behavior of Cu and its isotopes in the Yangtze River. Sci. Total Environ. 728, 138428 https://doi.org/10.1016/j.scitotenv.2020.138428.

Wiederhold, J.G., 2015. Metal stable isotope signatures as tracers in environmental geochemistry. Environ. Sci. Technol. 49 (5), 2606–2624. https://doi.org/10.1021/es504683e.

Xu, S., Frey, S.K., Erler, A.R., Khader, O., Berg, S.J., Hwang, H.T., Sudicky, E.A., 2021. Investigating groundwater-lake interactions in the Laurentian Great Lakes with a fully-integrated surface water-groundwater model. J. Hydrol. 594, 125911 https://doi.org/10.1016/j.jhydrol.2020.125911.

Yang, T., Chen, Y., Zhou, S., Li, H., 2019. Impacts of aerosol copper on marine phytoplankton: a review. Atmosphere 10 (7), 1–21. https://doi.org/10.3390/atmos10070414.

Yin, N.H., Sivry, Y., Benedetti, M.F., Lens, P.N.L., Hullebusch, E.D., 2015. Application of Zn isotopes in environmental impact assessment of Zn-Pb metallurgical industries: a mini review. Appl. Geochem. 64, 128–135. https://doi.org/10.1016/j.apgeochem.2015.09.016.

Zhao, Y., Liu, S.A., Xue, C., Mathur, R., Symons, D.T.A., Ke, J., 2022. Copper isotope fractionation in magmatic Ni–Cu mineralization systems associated with the variation of oxygen fugacity in silicate magmas. Geochim. Cosmochim. Acta 338, 250–263. https://doi.org/10.1016/j.gca.2022.09.040.